

**THE EFFECT OF OXIDATION TREATMENT OF MWCNT ON THE  
PROPERTIES OF PDMS NANOCOMPOSITE**

**by**

**NORKHAIRUNNISA BINTI MAZLAN**

**Thesis submitted in fulfillment of the requirements  
for the Degree of  
Doctor of Philosophy**

**May 2012**

## ACKNOWLEDGEMENTS

First and foremost, I would like to convey my heartiest appreciation to Dean of School of Materials and Mineral Resources Engineering, Prof. Ahmad Fauzi b Mohd Noor for his vital encouragement and support during my studies at the school. I also would like to express my great appreciation to my research supervisor, Assoc. Prof. Dr. Azizan Aziz, for his patient guidance, encouragement, useful critics and constructive suggestions during the planning and development of this research work. His willingness to give his time was really appreciated. My grateful thanks are also extended to Assoc. Prof. Dr. Ir. Mariatti Jaafar (co-supervisor) for her advice and knowledge towards making this research success especially in nanocomposite work and to Prof. Hanafi Ismail (co-supervisor) for his support encouragement and advice to complete this study.

Besides that, I would like to thank Ministry of Science, Technology and Innovation (MOSTI) for providing scholarship for me to pursue this study and Universiti Sains Malaysia for providing the facilities and financial support for this project under Universiti Sains Malaysia-Research University-Postgraduate Research Grant Scheme (USM-RU-PRGS) and USM Fellowship. In addition, I also would like to thank Intel Technologies Sdn. Bhd. for providing financial support for this research project under Center of Research and Teaching (CORT) programme.

I would like to express my great thanks to various people especially to the experienced technical staff for their contribution to this project, from School of Materials and Mineral Resources Engineering (Mrs. Fong Lee Lee, Mr. Zulkurnain, Pn. Haslina, Mr. Gunasegaran, Mr. Shahril Amir, Mr. Mohd. Faizal, Mr. Mohammad, Mr.

Sharul Ami, Mr. Abdul Rashid, Mr. Muhammad Khairi, Pn. Hasnah, Mr. Mohd. Halim, Mr. Meor Mohamad Noh, Mr. Mohammad Azrul, Mr. Mohd. Azam, Mr. Mohd. Suhaimi, Mr. Mohamad Zaini), School of Biological Sciences (Pn. Jamilah, Pn. Nor Faizah, Mr. Muthu) and School of Physics (Ms. Siti Khadijah). Not forget to all administration staff in School of Materials and Mineral Resources Engineering office for their great help. On top of that, I also would like to thank all postgraduate fellow friends especially to fellow labmates who works in Metallurgy Lab (Ms Junidah Abdul Shukor, Ms Ong Pek Ling, Pn. Nik Roselina, Ms Rahayu Saniman, Ms. Noor Hifzana, Mr Chua Tze Ping, and Mr Khe Che Seong) for their help, support and interesting discussions in the lab.

I would like to dedicate this dissertation to my father (Mr. Mazlan b Hj Maaya), mother (Pn. Sapiah bt Abd Manan) and brother (Muhammad Afiq b Mazlan) for their great encouragement and support. Great thanks to my loving husband (Ahmad Farhan Fadzin) for being a good soulmate to me and making my life more interesting. Also to my sweet little boy (Ahmad Faiq Ahmad Farhan), your presence enrich my life. Last but not least, special thanks to my in laws family. I am grateful to have you all as my family member and I love you all so much.

***Norkhairunnisa Binti Mazlan***  
**(May 2012)**

## TABLE OF CONTENTS

Acknowledgements.....	ii
Table of Contents.....	iv
List of Tables.....	x
List of Figures.....	xiii
List of Abbreviations.....	xx
List of Symbols.....	xxii
Abstrak.....	xxiii
Abstract.....	xxv

### CHAPTER 1 - INTRODUCTION

1.1 Background of the Study.....	1
1.2 Problem Statement.....	4
1.3 Objectives of the Study.....	6
1.4 Project Overview.....	6

### CHAPTER 2 - LITERATURE REVIEW

2.1 Introduction.....	8
2.2 Carbon in General.....	8
2.2.1 Carbon Nanotube (CNT).....	10
2.2.1.1 Multi-walled Carbon Nanotube (MWCNT).....	11
2.3 CNT Chirality.....	12
2.4 CNT Production.....	13
2.5 Comparisons in Output Analysis between MWCNT and SWCNT.....	15

2.5.1	MWCNT as Preferred Filler in Composite.....	16
2.6	General Properties of CNT.....	17
2.6.1	Bending of CNT with Respect to Mechanical Properties .....	17
2.6.2	Electronic Structure and Electron Transport in CNT.....	18
2.6.3	Thermal Conductivity Behavior of CNT.....	21
	2.6.3.1 Effects of Different Tube Length and Tubes Chirality on Thermal Conductivity of CNT.....	22
2.7	Surface Treatment on CNT.....	23
2.7.1	Why Surface Treatment is Important on CNT ?.....	23
2.7.2	Types of Surface Treatment on CNT.....	24
2.7.3	Oxidative Treatment on CNT.....	29
	2.7.3.1 Formation of Defects on the Carbon Rings.....	30
	2.7.3.2 Opening the end-cap of CNT.....	32
	2.7.3.3 Formation of Functional Groups on CNT.....	35
	2.7.3.4 Effects of the Acid Oxidation on the CNT Length.....	38
	2.7.3.5 Removal of Catalyst in Oxidation Treatment.....	41
2.7.4	Thermal Properties of the Oxidized CNT.....	43
2.7.5	Drawback of Surface Treatment on CNT.....	45
2.8	Thermoset Elastomer: Silicone Rubber.....	45
2.8.1	Polydimethylsiloxane (PDMS).....	46
2.9	Processing of CNT/Polymer Composite .....	47
2.10	Properties of CNT/Polymer Composite.....	49
2.10.1	Mechanical Properties of CNT/Polymer Composite.....	52
	2.10.1.1 Effect of Aspect Ratio on the Mechanical Properties of CNT/Polymer Composite .....	57
2.10.2	Electrical Conductivity of CNT/Polymer Composite.....	59
	2.10.2.1 Effects of Processing on the Conductivity of CNT/Polymer Composite.....	63

2.10.2.2	Effects of Aspect Ratio on the Electrical Conductivity of CNT/Polymer Composites.....	67
2.10.3	Thermal Properties of CNT/Polymer Composite.....	70
2.10.3.1	Effects of Aspect Ratio on Thermal Conductivity of CNT/Polymer Composite.....	74
2.11	Summary.....	76

## CHAPTER 3 - MATERIALS AND METHODS

3.1	Introduction.....	77
3.2	Materials and Chemicals.....	77
3.2.1	Matrices.....	77
3.2.2	Fillers.....	78
3.2.3	Chemicals.....	79
3.3	Oxidative Treatment of MWCNT.....	81
3.4	Preparation of Composites.....	83
3.5	Characterizations.....	84
3.5.1	Functional Group Analysis by Fourier Transform Infrared (FTIR) Analysis.....	84
3.5.2	X-ray Photoelectron Spectroscopy (XPS) Analysis.....	84
3.5.3	Determination presence of oxide debris on the oxidized MWCNT.....	85
3.5.4	Acid Base Titration Analysis (Back Titration Analysis).....	85
3.5.5	Raman Spectroscopy Analysis.....	86
3.5.6	Thermal Stability Analysis by Thermogravimetry (TG).....	87
3.5.7	Transmission Electron Microscopy (TEM) Analysis.....	87
3.5.8	Filler Density Measurement.....	88
3.5.9	Elemental Analysis.....	88
3.5.10	Dispersibility Analysis.....	89

3.5.11	Measuring the Dispersibility and Stability of MWCNT in Solvent by UV-Visible Spectroscopy .....	89
3.5.12	Zeta Potential Analysis .....	90
3.5.13	Scanning Electron Microscopy (SEM) Analysis .....	90
3.5.14	Mechanical Properties .....	91
3.5.14.1	Tensile Test .....	91
3.5.14.2	Morphology of the Tensile Fractured Surface .....	91
3.5.14.3	Dynamic Mechanical Analysis (DMA) .....	92
3.5.15	Morphology of the Cross Section on the Nanocomposite .....	92
3.5.16	Crosslink Density and Swelling Measurement of Nanocomposite .....	92
3.5.17	Thermal Properties .....	94
3.5.17.1	Thermal Stability .....	94
3.5.17.2	Thermal Conductivity .....	94
3.5.18	Electrical Conductivity .....	95

## CHAPTER 4 - RESULTS AND DISCUSSION

4.1	Introduction .....	96
4.2	Effects of oxidation treatment using concentrated HNO <sub>3</sub> (nMWCNT) .....	97
4.2.1	FTIR analysis .....	97
4.2.2	XPS analysis .....	100
4.2.3	Titration analysis .....	110
4.2.4	Raman analysis .....	113
4.2.5	Thermal analysis .....	116
4.2.6	TEM analysis .....	119
4.2.7	Density analysis .....	123
4.2.8	Dispersibility analysis .....	124

4.3	Effects of oxidation treatment using mixture of $\text{HNO}_3/\text{H}_2\text{SO}_4$ with ratio of 3:1 (nsMWCNT).....	132
4.3.1	FTIR analysis.....	132
4.3.2	XPS analysis.....	135
4.3.3	Titration analysis.....	143
4.3.4	Raman analysis.....	143
4.3.5	Thermal analysis.....	145
4.3.6	TEM analysis.....	147
4.3.7	Density analysis.....	148
4.3.8	Dispersibility analysis.....	149
4.4	Summary on the oxidative treatment on multiwalled carbon nanotubes.....	154
4.5	Investigation on the properties of PDMS reinforced with MWCNT oxidized in concentrated $\text{HNO}_3$ .....	159
4.5.1	Bonding properties.....	164
4.5.2	Mechanical properties.....	168
4.5.3	Morphology analysis.....	171
4.5.4	Dynamic Mechanical properties.....	179
4.5.5	Swelling and Crosslink properties.....	183
4.5.6	Thermal Stability properties.....	186
4.5.7	Thermal and Electrical Conductivity properties.....	189
4.6	Investigation on the properties of PDMS reinforced with MWCNT oxidized in acid mixture $\text{HNO}_3/\text{H}_2\text{SO}_4$ .....	192
4.6.1	Bonding properties.....	192
4.6.2	Mechanical properties.....	195
4.6.3	Morphology analysis.....	199
4.6.4	Dynamic Mechanical analysis.....	204
4.6.5	Swelling and Crosslink properties.....	208



4.6.6	Thermal Stability properties.....	210
4.6.7	Thermal and Electrical Conductivity properties.....	213
4.7	Summary on the properties of PDMS filled with oxidized MWCNT.....	215
CHAPTER 5 - CONCLUSIONS AND RECOMMENDATIONS		
5.1	Conclusions.....	220
5.2	Recommendations for Future Research.....	222
REFERENCES.....		224
APPENDICES		
APPENDIX A	The calculation of acid base titration.....	245
APPENDIX B	The calculation of MWCNT and PDMS matrix content.....	248
APPENDIX C	SEM images on raw and oxidized MWCNT.....	252
APPENDIX D	EDX analysis of raw and oxidized MWCNT.....	259
APPENDIX E	FTIR spectra of PDMS nanocomposite.....	260
APPENDIX F	Properties of 0.5 vol% to 2.0 vol% MWCNT/PDMS nanocomposites.....	264
APPENDIX G	Properties of 0.5 vol% and 2.0 vol% nMWCNT/PDMS and nsMWCNT/PDMS nanocomposites.....	265
LIST OF PUBLICATIONS.....		267

## LIST OF TABLES

		<b>Page</b>
Table 2.1	Electrical and mechanical characteristics of carbon nanotubes (Hoenlein <i>et al.</i> , 2003).	17
Table 2.2	Sidewall functionalization reactions on the nanotubes (Liu, 2008).	26
Table 2.3	Effects of the cutting method on CNT length.	40
Table 2.4	Effects of oxidized MWCNT filled nanocomposites on properties in various types of polymer matrix.	50
Table 3.1	Properties of polydimethylsiloxane (PDMS).	78
Table 3.2	Properties of Multiwall Carbon Nanotubes (MWCNT).	79
Table 3.3	List of chemicals and their properties which are related to this work.	80
Table 3.4	Oxidative treatment on MWCNT at different time treatment.	82
Table 3.5	Oxidative treatment on MWCNT at different temperature treatment.	82
Table 4.1	Assignment of IR spectra adsorption for raw MWCNT and nMWCNT.	100
Table 4.2	The XPS atomic (%) composition of raw MWCNT and nMWCNT and their percentage (%) intensity of C, O and N elements.	110
Table 4.3	Concentration of acidic sites based on titration analysis for raw MWCNT and nMWCNT.	112
Table 4.4	Comparison between previous results and present study on concentration of acidic sites.	113
Table 4.5	The intensity of D, G and G' band for raw MWCNT and nMWCNT	115
Table 4.6	Weight remained (wt%) and weight remove of functional groups (wt%) at 500°C for raw MWCNT and nMWCNT samples after decomposition at certain temperature.	119
Table 4.7	Density of raw MWCNT and nMWCNT.	124

Table 4.8	Absorbance value from UV-vis measurement and zeta potential at pH 7 for raw MWCNT and nMWCNT.	127
Table 4.9	Assignment of IR spectra adsorption of nsMWCNT.	133
Table 4.10	The XPS atomic (%) composition of nsMWCNT and their percentage (%) intensity of C, O and N elements.	142
Table 4.11	Concentration of acidic sites based on titration analysis for nsMWCNT.	143
Table 4.12	The intensity of D, G and G' band for nsMWCNT.	145
Table 4.13	Weight remained (wt%) and weight remove of functional groups (wt%) at 500°C for nsMWCNT samples after decomposition at certain temperature.	146
Table 4.14	Density of MWCNT nsMWCNT.	149
Table 4.15	Absorbance value from UV-vis measurement and zeta potential at pH 7 for nsMWCNT.	152
Table 4.16	Properties of raw MWCNT, oxidative nMWCNT and nsMWCNT.	157
Table 4.17	Properties of oxidative treatment on CNT done by other researchers	158
Table 4.18	Elemental composition of 80MWCNT6/PDMS nanocomposite.	167
Table 4.19	Summary of DMA results of control PDMS and PDMS filled with MWCNT and nMWCNT.	182
Table 4.20	Swelling ratio and crosslink density of control PDMS and PDMS filled with MWCNT and nMWCNT.	185
Table 4.21	Summary of TGA result of control PDMS and PDMS filled with MWCNT and nMWCNT.	188
Table 4.22	Thermal conductivity and electrical conductivity of control PDMS and PDMS filled with MWCNT and nMWCNT.	191
Table 4.23	Elemental composition of 31_140MWCNT6/PDMS nanocomposite.	195
Table 4.24	Summary of DMA results of PDMS filled oxidized nsMWCNT.	207

Table 4.25	Swelling ratio and crosslink density of PDMS filled nsMWCNT.	210
Table 4.26	Summary of TGA result of PDMS filled nsMWCNT.	213
Table 4.27	Thermal conductivity and electrical conductivity of PDMS filled nsMWCNT.	214
Table 4.28	Properties of PDMS filled with nMWCNT and nsMWCNT.	217
Table 4.29	Properties of MWCNT/PDMS observed by other researcher.	219

## LIST OF FIGURES

		Page
Figure 2.1	Carbon nanoworld based on the different types of hybridization, utilizing the bottom up approach (Popov, 2006).	10
Figure 2.2	Schematic of individual sheet of graphene and rolled graphene in order to form a carbon nanotube (Endo <i>et al.</i> , 2004).	11
Figure 2.3	Schematic image on the growth of the carbon nanotube. Blue cages indicate the carbon nanotubes. Red balls indicate catalytic particles (Hayashi <i>et al.</i> , 2003).	11
Figure 2.4	Multi walled carbon nanotubes (MWCNT) (Merkoçi, 2006).	12
Figure 2.5	Chirality of carbon nanotube (a) armchair (n, m) - (5, 5); (b) zigzag (n, m) – (9, 0); and (c) (n, m) – (10, 5) (Harris, 2004).	13
Figure 2.6	CNT production by arc discharge (Eichhorn and Stolle, 2008).	14
Figure 2.7	CNT production by laser ablation (Eichhorn and Stolle, 2008).	14
Figure 2.8	CNT production by CVD (Eichhorn and Stolle, 2008).	15
Figure 2.9	Comparison of structures, microscopy images and Raman spectrum between SWCNT and MWCNT (Valcárcel <i>et al.</i> , 2007).	16
Figure 2.10	Schematic images on electron transfer in metal, semiconductor and graphite in order to determine the electrical properties of the materials (Collins and Avouris, 2000).	19
Figure 2.11	Schematic drawing on metallic and semiconducting of (a) straight nanotubes and (b) twisted nanotubes (Collins and Avouris, 2000).	20
Figure 2.12	Thermal conductivity versus tube length (Sinnott and Aluru, 2006).	23
Figure 2.13	Non covalent treatment of hydrolyzed poly(styrene-co-maleic anhydride) (HSMA) with CNT (Xue <i>et al.</i> , 2008).	25
Figure 2.14	Oxidation treatment with strong acids.	26

Figure 2.15	Location attack on the unsaturated carbon during oxidation process (Zhang <i>et al.</i> , 2003).	30
Figure 2.16	An individual nanotube. Red circle color indicate the closed end cap of the nanotube (Silverman, 2005).	32
Figure 2.17	TEM images of opened end capped of carbon nanotubes after oxidation treatment with (a) boiling with HNO <sub>3</sub> , (b) boiling with KMnO <sub>4</sub> , (c) HF/BF <sub>3</sub> at room temperature and (d) OsO <sub>4</sub> in H <sub>2</sub> O at room temperature (Satishkumar <i>et al.</i> , 1996).	34
Figure 2.18	Opening of the tubes followed by layer by layer thinning on the tube structure (Ajayan <i>et al.</i> , 1993).	35
Figure 2.19	Step-wise progression mechanism on oxidation of CNT (Yue <i>et al.</i> , 1999).	36
Figure 2.20	Mole percent of –COOH groups versus oxidation or cutting time (Marshall <i>et al.</i> , 2006).	38
Figure 2.21	Average length of MWCNT oxidized at various oxidation (a) temperature, and (b) time (Hong <i>et al.</i> , 2007).	41
Figure 2.22	Thermal conductivity of carbon nanotubes versus fraction of functionalized atoms (Sinnott and Aluru, 2006).	43
Figure 2.23	Schematic chain of polydimethylsiloxane structure.	47
Figure 2.24	A molecular model of a CNT embedded in two layers of polymer. Extra energy is needed in order to pull the CNT through the interlock. A is point of entry and B is near-pullout position (Wong <i>et al.</i> , 2003).	54
Figure 2.25	Interfacial shear strength of the composite versus nanotube radius (Barber <i>et al.</i> , 2004).	57
Figure 2.26	Tensile strength and strain at break for different aspect ratio of MWCNT (Ayatollahi <i>et al.</i> , 2011).	58
Figure 2.27	A schematic model of isolated and bundled carbon nanotubes embedded in PDMS matrix.	61
Figure 2.28	Potential energy of interaction between two charged particles (Flandin <i>et al.</i> , 1999).	64

Figure 2.29	Schematic of CNT-reinforced polymer nanocomposites containing a) perfectly dispersed cylindrical CNTs, b) CNTs in the form of agglomerates and c) a mixture of individual CNTs and agglomerates (Li <i>et al.</i> , 2007).	66
Figure 2.30	Plot of electrical conductivity of the composite versus CNT content with different mean nanotube length (Martin <i>et al.</i> , 2004).	69
Figure 2.31	(a) Plot of electrical conductivity versus volume fraction of MWCNT, TEM images of (b) MWCNT with aspect ratio of 50, and (c) MWCNT with aspect ratio of 500 (Dang <i>et al.</i> , 2008).	70
Figure 2.32	SEM images of conductive particles and estimated particle packing by considering the aspect ratio of the fillers. (a) aluminium nitride, (b) silicone nitride and (c) multiwalled carbon nanotubes (Lee <i>et al.</i> , 2005).	74
Figure 2.33	Thermal conductivity of different filler versus filler content (Gojny <i>et al.</i> , 2006).	75
Figure 3.1	Schematic presentation on chemical structure Part A and Part B in PDMS.	78
Figure 3.2	Schematic diagrams for oxidative treatment of MWCNT in acid.	81
Figure 3.3	Flow chart of making composite.	83
Figure 3.4	Setup for titration analysis.	86
Figure 3.5	Schematic drawing of insertion of samples and hot disk sensor for thermal analyzer.	95
Figure 4.1	FTIR spectra of raw MWCNT and nMWCNT.	99
Figure 4.2	High resolution of XPS spectra of (a) C1s and (b) O1s for raw MWCNT.	101
Figure 4.3	High resolution XPS spectra of (a) C1s and (b) O 1s for 80MWCNT3 sample.	103
Figure 4.4	High resolution XPS spectra of (a) C1s and (b) O 1s for 80MWCNT6 sample.	104

Figure 4.5	High resolution XPS spectra of (a) C1s and (b) O 1s for 140MWCNT6 sample.	106
Figure 4.6	XP N1s spectra of 80MWCNT6 and 140MWCNT6 samples.	107
Figure 4.7	Possible acidic groups created on the surface of MWCNT.	111
Figure 4.8	Raman spectra of MWCNT with respect to purity and defects presence on the raw MWCNT and nMWCNT.	115
Figure 4.9	TG thermogram on weight loss vs temperature of the raw MWCNT and nMWCNT.	118
Figure 4.10	TEM image comparison between raw and oxidize MWCNT.	120
Figure 4.11	TEM image of 80MWCNT3 sample.	121
Figure 4.12	TEM image of 80MWCNT6 sample.	122
Figure 4.13	TEM image of 140MWCNT6 sample.	123
Figure 4.14	Dispersibility analysis of raw MWCNT and nMWCNT in water.	126
Figure 4.15	UV-Vis spectra of the raw MWCNT and nMWCNT.	127
Figure 4.16	Schematic drawing on dispersibility of untreated and oxidized MWCNT in water.	129
Figure 4.17	FTIR spectra of nsMWCNT.	134
Figure 4.18	High resolution of XPS spectra of (a) C1s and (b) O1s for 31_80MWCNT3 sample.	135
Figure 4.19	High resolution of XPS spectra of (a) C1s and (b) O1s for 31_80MWCNT6 sample.	137
Figure 4.20	High resolution of XPS spectra of (a) C1s and (b) O1s for 31_140MWCNT6 sample.	138
Figure 4.21	XP N1s spectra of nsMWCNT.	140



Figure 4.22	Oxidation debris solution originated from washing of (a) 140MWCNT6 and (b) 31_140MWCNT6 samples.	142
Figure 4.23	Comparison of Raman spectra with respect to purity and defects presence on the nsMWCNT.	144
Figure 4.24	TG thermogram on weight loss vs temperature of the nsMWCNT.	146
Figure 4.25	TEM micrograph for 31_80MWCNT6 sample.	147
Figure 4.26	TEM micrograph for 31_140MWCNT6 sample.	148
Figure 4.27	Dispersibility analysis of nsMWCNT in water.	150
Figure 4.28	UV-vis spectra of nsMWCNT.	151
Figure 4.29	Schematic presentation on reaction between 2 parts to form PDMS network.	159
Figure 4.30	Schematic presentation of covalent bonding between PDMS chain and hydroxyl groups on oxidized MWCNT.	160
Figure 4.31	Schematic presentation of covalent bonding between PDMS chain and carboxylic groups on oxidized MWCNT.	161
Figure 4.32	Schematic presentation of hydrogen bonding between PDMS chain and carboxylic groups on oxidized MWCNT.	162
Figure 4.33	Schematic drawing of hydrogen bonding between PDMS chain and carbonyl group of oxidized MWCNT.	163
Figure 4.34	Schematic drawing of hydrogen bonding between trimethylsiloxysilicate of PDMS chain and carbonyl group of oxidized MWCNT.	164
Figure 4.35	XPS spectra for the 80MWCNT6/PDMS nanocomposite. Deconvolution of (a) C1s, (b) O1s, and (c) Si 1s XPS spectrum.	165
Figure 4.36	Tensile strength of control PDMS and PDMS filled with MWCNT and nMWCNT.	169
Figure 4.37	Elongation at break of control PDMS and PDMS filled with MWCNT and nMWCNT.	170

Figure 4.38	Stress strain behavior of control PDMS and PDMS filled with MWCNT and nMWCNT.	171
Figure 4.39	SEM morphology on the tensile fractured surface of untreated MWCNT/PDMS nanocomposite at (a) 100X, (b) 2KX and (c) 30KX magnifications.	172
Figure 4.40	SEM morphology on the tensile fractured surface of 80MWCNT3/PDMS nanocomposite at (a) 100X, (b) 2KX and (c) 30KX magnifications.	174
Figure 4.41	SEM morphology on the tensile fractured surface of 80MWCNT6/PDMS nanocomposite at (a) 100X, (b) 2KX and (c) 30KX magnifications.	176
Figure 4.42	SEM morphology on the tensile fractured surface of 140MWCNT6/PDMS nanocomposite at (a) 100X, (b) 2KX and (c) 30KX magnifications.	177
Figure 4.43	TEM photo on the cross section of 140MWCNT6/PDMS nanocomposites.	179
Figure 4.44	Variation of storage modulus ( $E'$ ) versus temperature ( $^{\circ}\text{C}$ ) of control PDMS and PDMS filled with MWCNT and nMWCNT.	181
Figure 4.45	Variation of tan delta versus temperature of control PDMS and PDMS filled with MWCNT and nMWCNT.	183
Figure 4.46	Swelling versus time of control PDMS and PDMS filled with MWCNT and nMWCNT.	184
Figure 4.47	TGA spectra of control PDMS and PDMS filled with MWCNT and nMWCNT.	188
Figure 4.48	DTG spectra of control PDMS and PDMS filled with MWCNT and nMWCNT.	188
Figure 4.49	Schematic drawing of intermolecular hydrogen bonding among hydroxyl groups on MWCNT.	192
Figure 4.50	XPS spectra for the 31_140MWCNT6/PDMS nanocomposite. Deconvolution of (a) C1s, (b) O1s, and (c) Si1s XPS spectrum.	193
Figure 4.51	Tensile strength of PDMS filled with nsMWCNT.	196

Figure 4.52	Elongation at break of PDMS filled with nsMWCNT.	197
Figure 4.53	Stress strain behavior of PDMS filled with nsMWCNT	198
Figure 4.54	SEM morphology on the fractured surface of 31_80MWCNT3/PDMS nanocomposite at (a) 100X, (b) 2KX and (c) 30KX magnifications.	199
Figure 4.55	SEM morphology on the fractured surface of 31_80MWCNT6/PDMS nanocomposite at (a) 100X, (b) 2KX and (c) 30KX magnifications.	201
Figure 4.56	SEM morphology on the fractured surface of 31_140MWCNT6/PDMS nanocomposite at (a) 100X, (b) 2KX and (c) 30KX magnifications.	203
Figure 4.57	Variation of Storage Modulus (E') versus temperature (°C) of PDMS filled nsMWCNT.	206
Figure 4.58	Variation of tan delta versus temperature of PDMS filled nsMWCNT.	208
Figure 4.59	Swelling versus time of PDMS filled nsMWCNT.	209
Figure 4.60	TGA spectra of PDMS filled nsMWCNT.	211
Figure 4.61	DTG spectra of PDMS filled nsMWCNT.	212

## LIST OF ABBREVIATIONS

AlBN	: Azobisisobutyronitrile
BF <sub>3</sub>	: Boron trifluoride
CVD	: Chemical Vapor Deposition
DMA	: Dynamic mechanical analysis
DTA	: Dynamic thermal analysis
DWCNT-NH <sub>2</sub>	: Amino functionalized Double walled Carbon Nanotube
EDX	: Energy Dispersive X-ray
FE-SEM	: Field emission scanning electron microscope
FTIR	: Fourier transform infrared
HCl	: Hydrochloric acid
HF	: Hydrogen fluoride
HNO <sub>3</sub>	: Nitric acid
HSMA	: Hydrolyzed Poly(styrene-co-maleic anhydride)
HSO <sub>4</sub> <sup>-</sup>	: Bisulfate ion
H <sub>2</sub> O <sub>2</sub>	: Hydrogen peroxide
H <sub>2</sub> SO <sub>4</sub>	: Sulphuric acid
H <sub>3</sub> O <sup>+</sup>	: Hydronium ion
iPP	: Isotactic polypropylene
KBr	: Potassium bromide
KmnO <sub>4</sub>	: Potassium permanganate
MMA	: Methyl methacrylate
MWCNT-NH <sub>2</sub>	: Amino functionalized Multi walled Carbon Nanotube
Nmwcnt	: MWCNT oxidized in nitric acid
nsMWCNT	: MWCNT oxidized in acid mixture
NaClO	: Sodium hypochlorite

NO <sub>2</sub> <sup>+</sup>	: Nitronium ion
NaOH	: Sodium hydroxide
OsO <sub>4</sub>	: Osmium tetroxide
PDMS	: Polydimethylsiloxane
PMAS	: Poly(styrene-co-maleic anhydride)-block-polystyrene
PMMA	: Polymethylmethacrylate
PP	: Polypropylene
PS	: Polystyrene
PTFE	: Polytetrafluoroethylene
PU	: Polyurethane
P3HT	: Poly(3-hexylthiophene)
RBM	: Radial breathing mode
SEM	: Scanning electron microscope
SLS	: Sodium lauryl sulfonate
TEM	: Transmission Electron Microscope
TGA	: Thermogravimetric analysis
TLCP	: Thermotropic liquid crystalline polymer
UV-vis	: Ultraviolet visible
XRD	: X-ray diffraction
XPS	: X-ray photoelectron spectroscopy

## LIST OF SYMBOLS

$\pi$	: Pie
$\sigma$	: Sigma
%	: Percent
at%	: Atomic percent
wt%	: Weight percent
vol%	: Volume percent
$T_g$	: Glass transition temperature
$E'$	: Storage modulus
$E''$	: Loss modulus
$l$	: Length
$d$	: Diameter
$D$	: Diameter of sphere
$k_f$	: Thermal conductivity of filler
$k_m$	: Thermal conductivity of matrix
$\rho_s$	: Density of sample
$m_s$	: Mass of sample
$v_s$	: Volume of sample
$\text{Ar}^+$	: Argon ion
$t$	: Sample thickness
$\Omega$	: Electrical resistance
$A$	: Area
$\rho$	: Density
$I_D$	: Intensity of D band
$I_G$	: Intensity of G band
$\delta$	: Tan delta (loss factor)

# KESAN RAWATAN PENGOKSIDAAN MWCNT KE ATAS SIFAT-SIFAT NANOKOMPOSIT PDMS

## ABSTRAK

MWCNT mempunyai sifat elektrik yang unik, kekonduksian terma yang lebih tinggi daripada berlian, and sifat mekanikal yang baik di mana kekuatan dan kekakuan melebihi bahan lain yang sedia ada. Walaubagaimanapun, kurangnya serakan dan pengikatan antaramuka antara MWCNT dan matrik polimer memberi satu cabaran dalam menghasilkan nanokomposit yang mempunyai sifat yang bagus. Rawatan pengoksidaan dilakukan ke atas MWCNT bagi menambahbaikkan serakan dan pengikatan antaramuka di antara nanotub dengan PDMS. Kefungsian pengoksidaan MWCNT dihasilkan melalui pengoksidaan menggunakan sama ada asid tunggal ( $\text{HNO}_3$ ) atau gabungan asid ( $\text{HNO}_3/\text{H}_2\text{SO}_4$ ) pada nisbah 3:1. Rawatan ini dilakukan pada tempoh masa (3 dan 6 jam) dan suhu ( $80^\circ\text{C}$  dan  $140^\circ\text{C}$ ) rawatan yang berbeza. Analisa FTIR dan XPS menunjukkan kehadiran pelbagai kumpulan berfungsi oksigen seperti C-O, C=O dan COOH. Nisbah kandungan O/C meningkat dari 0.17 bagi MWCNT yang tidak dirawat, kepada 0.56 bagi MWCNT yang teroksida. Pentitratan asid bes menunjukkan peningkatan kandungan kumpulan asid sebanyak 159%. Kesan pengoksidaan memberi kesan yang lebih ketara apabila suhu rawatan ditingkatkan kepada  $140^\circ\text{C}$  selama 6 jam sehinggakan nisbah  $I_D/I_G$  didapati meningkat dari 0.19 kepada 0.83 serta terdapat penurunan dalam kestabilan terma. Kewujudan kumpulan berfungsi menyebabkan pembentukan lapisan elektrik berganda pada permukaan MWCNT, lalu menghasilkan serakan yang baik di dalam air. Lapisan ini juga mampu mengatasi daya tarikan van der Waals antara nanotub, lalu menurunkan saiz gumpalan. Selain itu, kecacatan ke atas MWCNT dan kewujudan kumpulan pemangkin dapat dilihat melalui TEM. Bagi PDMS terisi

dengan MWCNT yang dirawat dengan  $\text{HNO}_3$  pada  $80^\circ\text{C}$  untuk 3 dan 6 jam, didapati kekuatan tensil meningkat kepada 5.06 MPa, manakala kekonduksian terma dan elektrik masing-masing meningkat sedikit kira-kira 24% dan 42% dibandingkan dengan nanokomposit MWCNT/PDMS yang tidak dirawat. Walaubagaimanapun bagi PDMS terisi dengan MWCNT yang dirawat pada suhu  $80^\circ\text{C}$  selama 6 jam di dalam gabungan asid, terdapat sedikit penurunan dalam sifat terma dan elektrik, masing-masing kepada 0.19 W.mK dan  $-4.62 \text{ Log/Scm}^{-1}$ . Penurunan lebih ketara bagi PDMS terisi MWCNT yang dirawat pada suhu  $140^\circ\text{C}$  selama 6 jam kerana terdapat penurunan nilai  $T_g$  sebanyak  $9^\circ\text{C}$  berbanding PDMS terisi dengan MWCNT yang telah dioksidakan pada  $80^\circ\text{C}$  selama 6 jam. Pengoksidaan yang terlampau ke atas MWCNT mengurangkan keupayaannya untuk membentuk ikatan antaramuka yang baik dengan matrik PDMS. Oleh itu, MWCNT jenis ini sesuai digunakan untuk meningkatkan sifat keplastikan pada matrix polimer.



# THE EFFECT OF OXIDATION TREATMENT OF MWCNT ON THE PROPERTIES OF PDMS NANOCOMPOSITE

## ABSTRACT

MWCNT have a unique electrical properties, thermal conductivity which is higher than diamond and a good mechanical properties where strength and stiffness exceed any other current materials. However, poor dispersibility and interfacial adhesion of MWCNT in polymer matrix presents a considerable challenge in developing nanocomposite with good properties. Oxidation treatment was done on MWCNT as to improve the dispersion and interfacial adhesion between the nanotubes and PDMS. The oxidation treatments of MWCNT were carried out by oxidizing using either single acid ( $\text{HNO}_3$ ) or mixture of acids ( $\text{HNO}_3/\text{H}_2\text{SO}_4$ ) at 3:1 ratio. The treatments were done for different period of time (3 and 6 hours) and temperature ( $80^\circ\text{C}$  and  $140^\circ\text{C}$ ). FTIR and XPS analysis showed the presence of various functional groups such as C-O, C=O and COOH. The O/C ratio increased from 0.17 for untreated MWCNT to 0.56 for oxidized MWCNT. Acid bes titration showed increase in concentration of acid groups about 159%. The oxidation affects the tubes more significantly when the temperature and time increased to  $140^\circ\text{C}$  and 6 hours respectively as the  $I_D/I_G$  ratio increased from 0.19 to 0.83 and reduction in thermal stability. The presence of functional groups formed electrical double layer on the MWCNT surface and thus, gave good dispersibility in water. This layer also overcome the strong van der Waals force within the nanotubes and reduced agglomeration. The presence of defects and catalysts were also observed by TEM. For PDMS filled with MWCNT oxidized in  $\text{HNO}_3$  at  $80^\circ\text{C}$  for 3 and 6 hours, the tensile strength increased to 5.06 MPa, while thermal and electrical conductivity slightly increased for approximately to 24% and 42%, respectively over the untreated

MWCNT/PDMS nanocomposites. However, for PDMS filled with MWCNT oxidized at 80°C for 6 hours in acid mixture, the thermal and electrical conductivities were slightly decreased to 0.19 W/mK and -4.62 Log/Scm<sup>-1</sup>. Decrease in properties was more significant for PDMS filled with MWCNT oxidized at 140°C for 6 hours as the  $T_g$  value decreased for 9°C compared PDMS reinforced with MWCNT oxidized at 80°C for 6 hours, in which its  $T_g$  was approximately -35°C. Aggressive oxidation treatment reduces the capability of MWCNT to form good interfacial interaction with the PDMS matrix. However, this type of MCWNT was suitable to be used to increase the plasticity of the polymer matrix.

## CHAPTER 1

### INTRODUCTION

#### 1.1 Background of the Study

Nanostructured materials play an important role in the past decade due to their wide range of potential applications in many areas such as in the field of aerospace (Taczak, 2006), actuators (Ashrafi *et al.*, 2006), biomedical (Ji *et al.*, 2010), electronics (Wang *et al.*, 2010), etc. One of the promising nanostructured materials is Multi-walled Carbon Nanotube (MWCNT) which can be utilized in various applications as reinforcing fillers especially in the field of polymer-based composites. High aspect ratio ( $l/d$ , where  $l$  is length and  $d$  is diameter) of CNT facilitates it to form network like structure in the composite. Moreover, its unique electronic properties, high structural flexibility and high mechanical strength make it stiffer and stronger materials than other potential materials such as graphene, diamond, carbon black, etc. Thus, various types of polymer have been embedded with CNT with a desire to fabricate new advanced materials as to enhance the composite properties.

Few reviews focusing on elastomer nanocomposites have been reported in recent years. Likozar and Major (2010), overviewed the distribution of MWCNT in the elastomer rubber matrix and found out that the presence of MWCNT improved the performance of the nanocomposites. In addition, degree of dispersibility and high aspect ratio of CNT affects the thermal conductivity of the elastomer filled MWCNT as investigated by Hong *et al.* (2010). Hikage *et al.*, (2007) analyze elastomer containing different fillers in order to develop a lightweight human phantom with

specific gravity below 1.0. While Bokobza and Kolodziej (2006), examined different level of reinforcement for elastomer contained different fillers.

Polydimethylsiloxane (PDMS) is one of the high performance silicone rubber elastomer with combination of high flexibility of  $-\text{[Si-O]}_x-$  chain segments with inherent strength of (Si-O) siloxane bonds, excellent thermal stability with slow heat release rates, low viscosity, low surface free energy, low toxicity and less chemical reactivity (Hamdani *et al.* (2009), Chaudhry and Billingham (2001), Mark (2004), Esteves *et al.* (2010)). Due to the high performance of PDMS material it may suitable to be combined with the versatile filler such as MWCNT. As we know, the CNT price in the market is too high. Thus, limit the use and exploration of CNT in research study. However, the CNT price has dropped dramatically over the past several years due to the efforts that focused on realizing mass production of CNT and its application in many field of industries.

Recent articles review on four requirements systems for effective reinforcement as mentioned by Coleman *et al.* (2006). These systems are (i) a large aspect ratio to maximize the load transfer to CNT, (ii) good dispersibility of individual CNT throughout the polymer matrix, (ii) randomness and alignment of CNT, and (iv) interfacial load transfer so as to achieve an efficient load transfer to the CNT network.

However, the as manufactured CNT exists as agglomerates of several hundred micrometers due to extremely high surface energy combined with impurities contamination create an obstacle to most applications. The tube surface not only

attracted to each other by van der Waals force but also due to their extremely high aspect ratio and high flexibilities increase the possibility of entanglements. Highly entangled CNT are difficult to disperse uniformly throughout the matrix. Moreover, agglomeration of CNT could not provide three-dimensional networks which are important in transport properties such as electrical and thermal conductivity. Poor interfacial strength of CNT and matrix in composite may cancel the uniformity of stress distributions and increase the stress concentration in the composite. The stress transfer occurred between matrix and nanotube at interface critically control the mechanical properties of the composites. Therefore, it is necessary to break the van der Waals force so as to get rid the CNT entanglements by shortening the CNT length. Apart from breaking the CNT entanglements, the impurities that might present in the as-prepared CNT were metal catalyst particles, amorphous carbon and other carbonaceous species. Monodispersity and high purity of CNT are essential for it to function as a reinforcing material.

However, there is still huge contrast between the promising potential and reality of using CNT in practical applications on a widespread scale. Up to date, there has not been a study that examine on the effect of different oxidation treatment of MWCNT in PDMS. The main goals of this work were first to functionalize the MWCNT with either  $\text{HNO}_3$  or mixture of  $\text{HNO}_3/\text{H}_2\text{SO}_4$  acids and investigated the outcome from the oxidation process. Both  $\text{HNO}_3$  and  $\text{HNO}_3/\text{H}_2\text{SO}_4$  acids are choose because they function as strong oxidizing agent and can provide more oxygen functional groups on the nanotube surface. Subsequently, the properties of the PDMS filled with oxidative MWCNT are determined.

## 1.2 Problem Statement

Due to the strong van der Waals force, high aspect ratio and high flexibility of CNTs, they tend to agglomerate and entangle among the tubes. This led to poor interfacial bonding between CNT and matrix. Therefore, it is necessary to break down the van der Waals force among CNT in order to reduce the entanglement/or agglomerations of the CNT in matrix. The CNT surface can be functionalized either by chemical (Datsyuk *et al.*, 2008) or physical (Wang *et al.*, 2003) treatments. Physical dispersion methods include ball milling, ultrasonication in selected solvent, grinding, and high speed shearing. These methods may disrupt the CNT structure by inducing severe damage on the tube walls. In chemical modification method, the CNT can be functionalized by covalent (Verdejo *et al.*, 2007) or non-covalent treatment (Wang *et al.*, 2008b). Covalent treatment is functionalizing the CNT surface with functional groups, while non-covalent treatment is surrounding or wrapping the CNT with polymer chain. These chemical methods also may give rise to CNT being damaged due to the strong acid treatment. Therefore, as stated above, combination of cutting and functionalization of CNT are good ways to have good dispersion of CNT in polymer matrix. In addition, the oxidation process can create defects on the CNT surface with abundance of functional groups on top of it. Thus, both CNT and matrix can have better interfacial bonding.

In order to improve the processability of CNT in polymer matrix, the CNT length needs to be loosened and shortened. At the same time the CNT needs to be oxidized as well so as to improve the CNT dispersibility and form strong interfacial bonding between CNT and polymer matrix. The oxidation process also led to reduction in length of the CNT and affect the size distribution as well.

The raw (as produced) CNT contained many impurities such as metal catalyst and amorphous carbon. Presence of these unwanted materials might reduce the properties of the composite as well. Oxidation process might help in diminish or reduce these unwanted materials.

It is evident from many studies that the presence of oxygenated functional groups on the CNT serves as starting point for binding with the polymer matrix. Besides that, defects created on the CNT surface during the oxidation process can tailor the CNT surface for desired applications. The CNT is more reactive at their tips and on the defects walls, thus enhanced the chemical reactivity.

The oxidation process on CNT need to be controlled in order to obtain CNT with adequate functional groups and optimum CNT length that is sufficient for composite applications to be realized. Datsyuk *et al.* (2008), reviewed on the different chemical oxidation treatment on MWCNT. Hong *et al.* (2007), examined the effects of different oxidative conditions on the properties of MWCNT in PP nanocomposites. Different mechanical and oxidative treatment on CNT in epoxy nanocomposites have been investigated by Li *et al.* (2007). Thus, it can be said that controlling the oxidation process may affect the intrinsic properties of the CNT, as well as the nanocomposite.

### **1.3 Objectives of the Study**

The functionalization of MCWNT is accomplished by oxidative acid treatment. The PDMS was reinforced with oxidized MWCNT. The objectives of this work are:

- a) To prepare and investigate the effects of different oxidative acid treatment on MWCNT at different time and temperature treatment.
- b) To study different properties between as-received MWCNT and functionalized MWCNT.
- c) To compare the properties of the unmodified MWCNT/PDMS nanocomposite with oxidative MWCNT/PDMS nanocomposite.
- d) To investigate the interactions between the oxidized MWCNT and PDMS matrix.

### **1.4 Project Overview**

In achieving the objectives, four main experiments were conducted. First and second experiment involved oxidized acid treatment on the MWCNT by  $\text{HNO}_3$  or  $\text{HNO}_3/\text{H}_2\text{SO}_4$  at  $80^\circ\text{C}$  with different treatment time and constant treatment time with different oxidized processing temperature, respectively. In this experiment, the outcome of the resulting oxidized MWCNT product were characterized so as to understand the effects of the different oxidative treatments. Density, dispersibility of CNT in distilled water, stability and quality of the CNT suspension, electrophoretic mobility of CNT, structural integrity of CNT, thermal stability, functional groups analysis, acid base titration analysis, and morphological analysis of the MWCNT was further investigated using characterization techniques mentioned in chapter three.



Moreover, properties between the as-received MWCNT and oxidized MWCNT were also evaluated.

Next, third and fourth experiments were conducted by embedding the resultant of the oxidized MWCNT from experiment one and three, respectively, in PDMS matrix. The mechanical, thermal, electrical, morphology and swelling properties of the cured unmodified MWCNT/PDMS and oxidative MWCNT/PDMS nanocomposites were identified. Moreover, selected nanocomposite were sent for XPS analysis so as to investigate presence of bonding between the oxidized MWCNT and PDMS matrix.

## **CHAPTER 2**

### **LITERATURE REVIEW**

#### **2.1 Introduction**

In this chapter, the review is focus on oxidation process of MWCNT since the aim of this study is to understand the effects of oxidized MWCNT on the PDMS nanocomposites. The purpose on the oxidation study is to understand the effect of functionalization on the nanotubes in hoping that the properties of the treated nanotubes is better than untreated nanotubes. The review focus more on oxidation treatment of MWCNT. Various effects on the oxidation process such as opening the end capped tubes, promoting the functional groups on the tubes surface, cutting the tube length, removal of catalyst in the tubes in or near the end tubes and thermal stability of the oxidative tubes were discussed.

Finally, the review focus on the silicone rubber filled with oxidized MWCNT, on mechanical, thermal and electrical properties of the nanocomposites. Overall, this chapter discussed on oxidation treatment used in this work and its effect on the properties of the MWCNT/ polymer composite.

#### **2.2 Carbon in General**

Carbon (C) was the sixth most abundant element exist in the universe. It provides the framework for all living creatures. The element can be found in the form of amorphous carbon, graphite, diamond, carbon 60, carbon nanotubes, buckminsterfullerenes and many more. Moreover, compound of carbon with other elements were also very common.

Carbon is also known to have four electrons in its valence shell. The core electrons is  $1s^2$  which is strongly bonded while the other four valence electrons are weakly bonded. Thus, each carbon atom can share electrons up to four different atoms and combine with another carbon atom or other elements. Owing to this fact, carbon can be in the form of various multi-atomic structures with different molecular configurations called allotropes. The allotropes involve hybridization process. Hybridization determined the chemical, physical and configurational properties of the carbon materials.

Figure 2.1 shows the carbon materials with different types of hybridization.  $sp$  hybridization can be observed in carbyne,  $sp^2$  hybridization is observed in graphite and  $sp^3$  hybridization is found in diamond (Popov, 2006). There were  $sp$ ,  $sp^2$  and  $sp^3$  hybridization as shown in Figure 2.1 which related to the carbon atom forming small organic molecules such as adamantane, ovalene and cumulene. Diversification from the organic molecules leads to the formation of the carbon nanofillers such as nanodiamond, fullerene, nanotubes and graphene. More complex unit of carbon can be form such as carbon onions, nanotubes (NT) ropes, MWNT, nanocarbon diamond (NCD) films, carbon fibers and carbon black with bigger structure size of the carbon nanofillers. Carbon nanofillers are defined as a material that built at nanometer scale ranging from fullerenes, carbon nanotubes to nanoporous materials (Endo *et al.*, 2004).

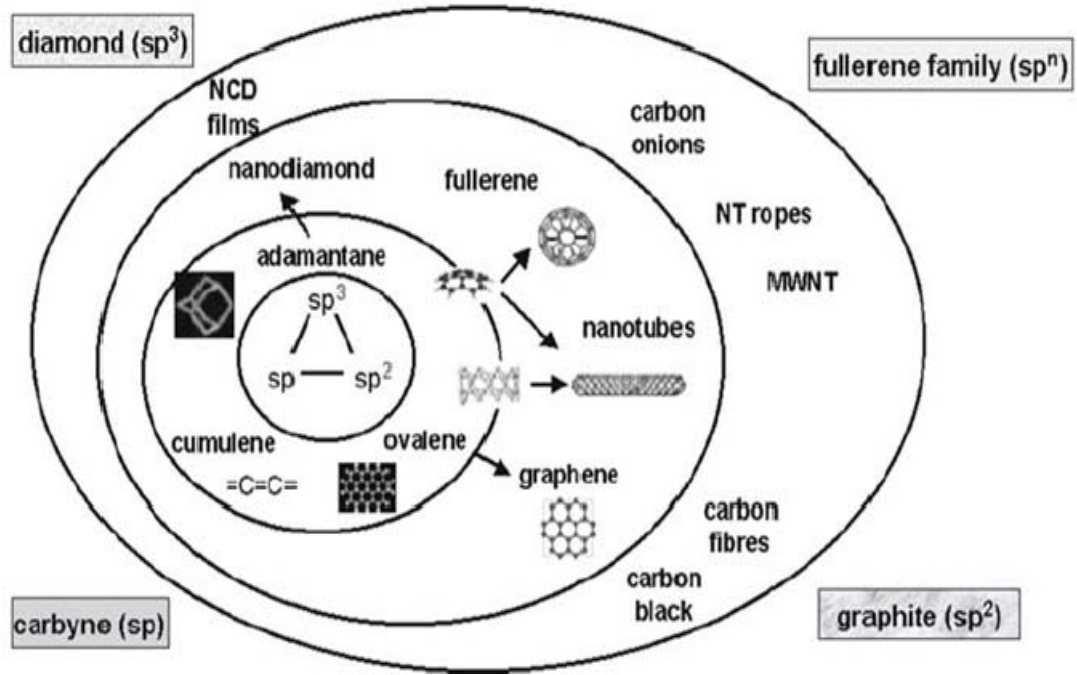


Figure 2.1 Carbon nanoworld based on the different types of hybridization, utilizing the bottom up approach (Popov, 2006).

### 2.2.1 Carbon Nanotube (CNT)

Carbon Nanotubes (CNTs) were first discovered by Japanese electron microscopist Sumio Ijima in 1991 (Ijima S, 1991). He found a graphitic structure including nanoparticles and nanotubes that had never been observed before (Arben, 2006). Figure 2.2 shows the schematic of individual sheet of graphene and rolled graphene to form CNT. CNT can be thought as a single graphite layer that is rolled up to make a seamless hollow cylinder (Endo *et al.*, 2004). It consists of a variety of diameter in nanosized with many microns in length. CNTs with only one carbon sheet are named single-walled carbon nanotubes (SWCNTs) while CNT with multi layer of graphene rolls are known as Multi-Walled Carbon Nanotubes (MWCNT). Jeykumari and Narayanan (2009) noted that MWCNT usually have diameter of 2 to 100 nm with 2 to 10 nm in internal diameter, while SWCNT have about 0.2 to 2 nm

in diameter. Hayashi *et al.* (2003), shows that the as-produced CNT usually have closed cap and catalyst that may exist at the end cap of the tube where the growth occurs as illustrate in Figure 2.3.

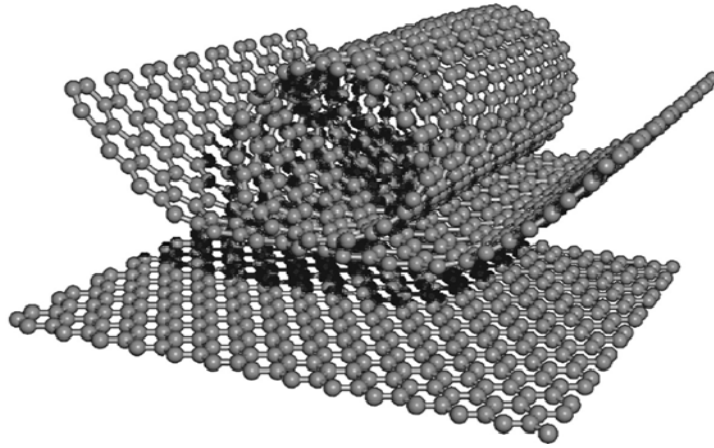


Figure 2.2 Schematic of individual sheet of graphene and rolled graphene in order to form a carbon nanotube (Endo *et al.*, 2004).

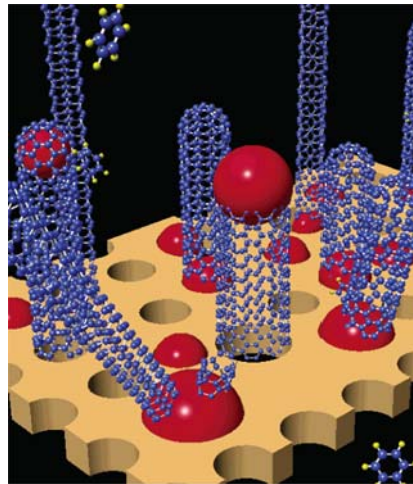


Figure 2.3 Schematic images on the growth of the carbon nanotube. Blue cages indicate the carbon nanotubes. Red balls indicate catalytic particles (Hayashi *et al.*, 2003).

#### 2.2.1.1 Multi-walled Carbon Nanotube (MWCNT)

Figure 2.4 shows that Multi-walled carbon nanotubes (MWCNTs) have several coaxial graphene (Merkoçi, 2006). The early structure was multiwall morphology consist of coaxial cylinders arranged in a “Russian doll” configuration.

Shanmugam and Gedanken (2006) have successfully created MWCNT with different shaped such as bamboo-shaped, straight and twisted MWCNT by pyrolysis process.

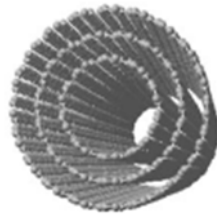


Figure 2.4 Multi walled carbon nanotubes (MWCNT) (Merkoçi, 2006).

According to Meyyapan (2005), when the graphene rolled over to form a CNT, the electrons get confined in particular direction, which insist on the formation of rehybridization. In rehybridization, three  $\sigma$ -bonds went slightly out of plane and the  $\pi$ -bond becomes more delocalized outside of the nanotubes. The three  $\sigma$ -bonds are responsible for the mechanical strength of the CNT while  $\pi$ -bond is accountable to the electronic and thermal properties of the CNT. The  $\pi$ -bonds are also responsible for the interaction between the layers in MWCNT and between SWCNTs in SWCNT bundle (Ruoff *et al.*, 2003).

### 2.3 CNT Chirality

CNT also was uniquely different from other types of filler. Despite its long tubular structure with hole in the middle, it has different tube chirality (Figure 2.5). According to Harris (2004), the ‘zigzag’ and ‘armchair’ refer to the arrangement of the hexagons around the circumference. As for the chiral structure, the hexagons are arranged helically around the tube axis.

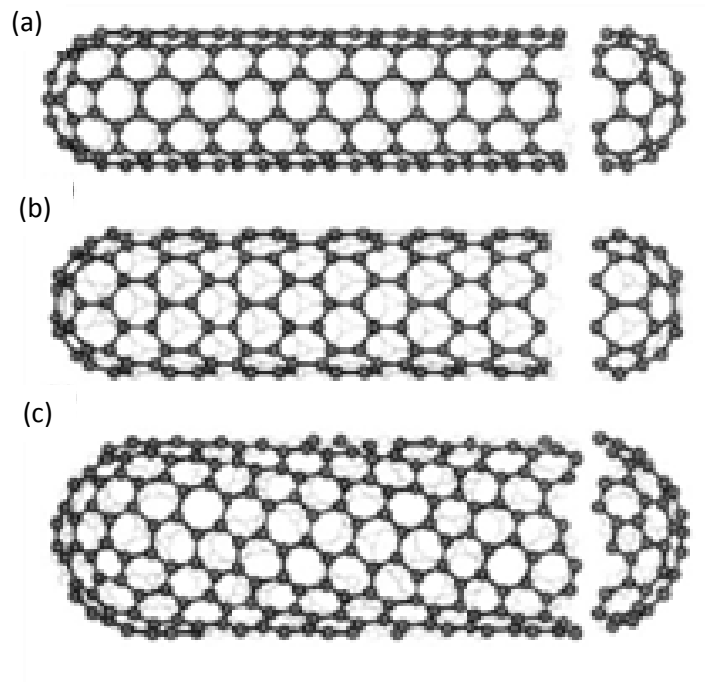


Figure 2.5 Chirality of carbon nanotube (a) armchair  $(n, m) - (5, 5)$ ; (b) zigzag  $(n, m) - (9, 0)$ ; and (c)  $(n, m) - (10, 5)$  (Harris, 2004).

## 2.4 CNT Production

The CNT is manufactured in many different ways and the CNT are produced along with different amount of catalyst impurities and amorphous carbon. There are three main methods used in the synthesis of CNT which are arc-discharge, laser ablation and chemical vapor deposition (CVD) as described by Eichhorn and Stolle (2008).

In arc discharge methods, the MWCNT is produced through arc-vaporization of two graphite rod placed end to end as represented in Figure 2.6. The chamber is filled with inert gas such as helium or argon at low pressure. Arc discharge techniques give the highest amount of catalyst particles while CVD technique was the least (Chaturvedi *et al.*, 2008). Thus this explained the drawback in using arc-discharge method which is more expensive because the need to remove the unwanted

metal catalyst and non-nanotube carbon from the as produced CNT. The presence of impurities and amorphous carbon will affect the mechanical properties of the composites (Schulte *et al.*, 2005).

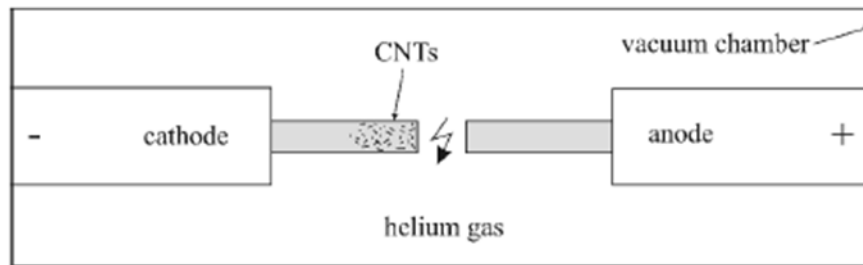


Figure 2.6 CNT production by arc discharge (Eichhorn and Stolle, 2008).

Figure 2.7 shows the production of CNT by laser ablation technique. The laserbeam was directed straight to the graphite target and vaporize it. The vaporized carbon particles move to copper collect vessel with aid by argon flow. This technique produces 70% of CNT by weight and mainly producing CNT with high tubes quality. The disadvantage with this technique is the high cost of operation due to demand of having high-powered laser.

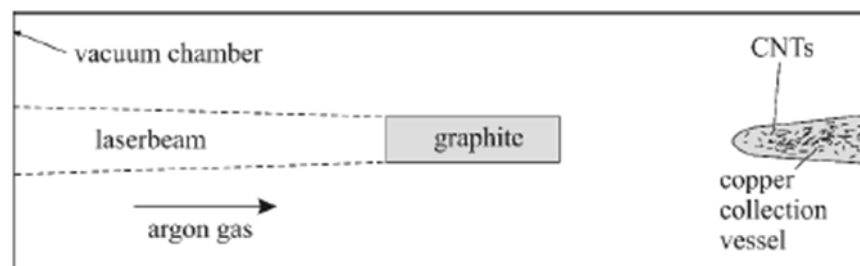


Figure 2.7 CNT production by laser ablation (Eichhorn and Stolle, 2008).

Both arc discharge and laser ablation techniques, are limited in volume sample and relatively high cost in producing the CNT. Thus, the limitations have motivated the the development of gas phase technique in producing CNT such as Chemical Vapor Deposition (CVD). In the CVD method (Figure 2.8), methane gases



was utilized as a source for carbon atoms combined with metal catalyst particles as seeds to support the growth of the nanotubes at relatively low temperatures (500-1000°C). The production of CNT can be up to 100% by weight. The advantage of CVD technique is, simple and favorable technique since the processing technique is cheap with less impurities on CNT.

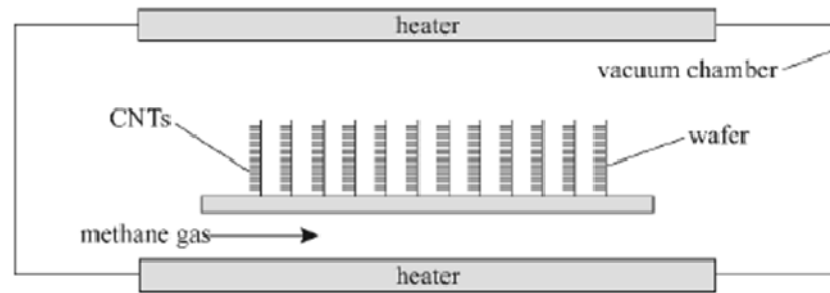


Figure 2.8 CNT production by CVD (Eichhorn and Stolle, 2008).

## 2.5 Comparisons in Output Analysis between MWCNT and SWCNT

The structure of the MWCNT and SWCNT can be differentiated by observation under electron microscopy and Raman analysis (Valcárcel *et al.*, 2007). Figure 2.9 shows that SWCNT consist of only single wall layer while MWCNT have multiple layers of wall. From electron microscopy, it can be seen that strong interaction between neighboring SWCNT is due to the van der Waals force, which make the SWCNT packed into thick bundle or ropes.

In Raman spectrum, both SWCNT and MWCNT have D and G bands. The D band associates to the disorder graphite while G band refer to the degree of graphitization of the CNT. The difference between SWCNT and MWCNT in Raman analysis lies on the third mode named radial breathing mode (RBM). The intensity of RBM is dependent on the diameter of CNT (Eichhorn and Stolle, 2008). This RBM band which is significantly appear in SWCNT while for MWCNT, the RBM band

appears only if the MWCNT have small diameter in few nanometers (Ando *et al.*, 1999). The RBM signals was near  $100\text{-}300\text{cm}^{-1}$  which indicate changes in diameter distribution (Seifi *et al.*, 2007).

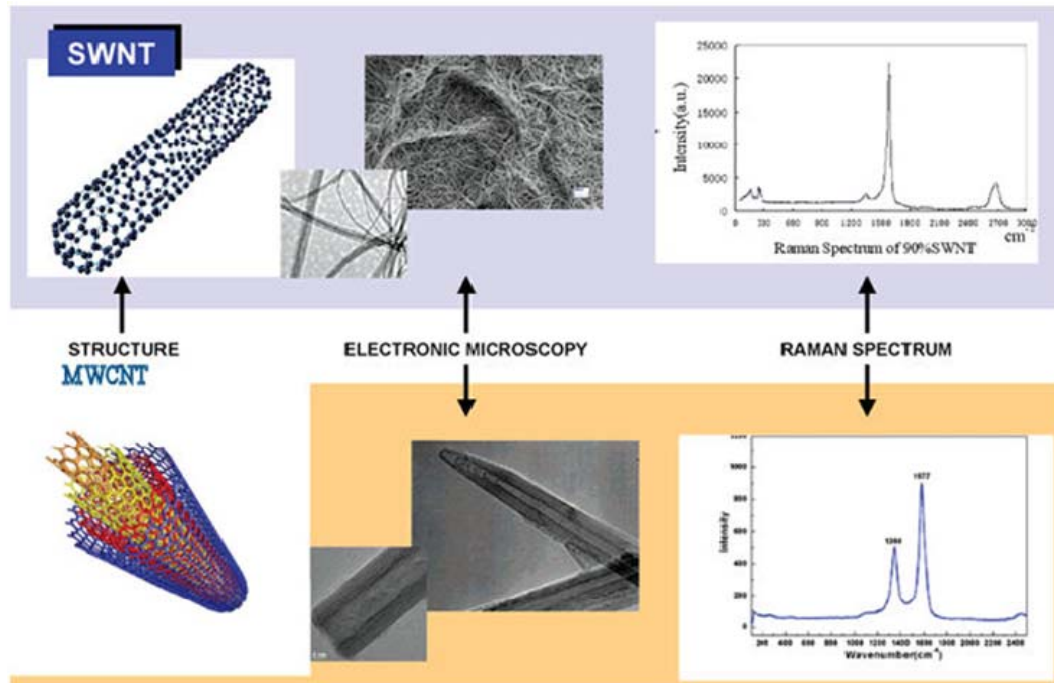


Figure 2.9 Comparison of structures, microscopy images and Raman spectrum between SWCNT and MWCNT (Valcárcel *et al.*, 2007).

### 2.5.1 MWCNT as Preferred Filler in Composite

There are few reasons on selecting MWCNT as filler in composite rather than SWCNT. It is not only due to the low cost of production but also due to the physical properties of the MWCNT itself. The MWCNT are more rigid than SWCNT because they consist of several rolls of graphene sheet that make it more stable than SWCNT. MWCNT also can act as carbon micro- or nanoparticles. In addition, only low loading of MWCNT is needed in order to achieve percolation threshold. Thus, MWCNT can exhibit excellent mechanical, thermal and electrical properties. Moreover their aspect ratio is as high as 1000, which can induce better interfacial interaction with the polymer matrix (Bikiaris *et al.*, 2008). In order to improve interaction between filler and matrix, CNT might be required to be treated and

functionalized. The SWCNT is not suitable for oxidative treatment. This is because those SWCNTs are so small and hence not protected by outer layers. By creating defects on the SWCNT surface, the tubes will collapse spontaneously due to their instability during the process (Ago and Yamabe, 1999).

## 2.6 General Properties of CNT

CNT have been intensively studied by most researchers due to the low density of the tubes and offer better mechanical, thermal and electrical properties as reinforcing filler in the composite. The diameter of the tubes can be as small as 0.4nm. The aspect ratio can be very large which are greater than  $10^4$ . CNT have  $sp^2$  bonding which consists of one  $\sigma$ -orbital and two  $\pi$ -orbital are hybridized and take part in covalent bonding. The  $sp^2$  bonds can make the nanotubes stiff and strong in nature. Nanotubes exhibit a remarkable electronic and mechanical characteristic, as summarized by Hoenlein *et al.* (2003) in Table 2.1.

Table 2.1 Electrical and mechanical characteristics of carbon nanotubes (Hoenlein *et al.*, 2003).

Electrical Conductivity	Metallic or semiconducting
Electrical Transport	Ballistic, no scattering
Maximum current density	$\sim 10^{10}$ A/cm <sup>2</sup>
Maximum strain	0.11% at 1 kV
Thermal Conductivity	6000 W/mK
Diameter	1 to 100 nm
Length	Up to millimeters
Gravimetric surface	$>1500$ m <sup>2</sup> /g
<i>E</i> -modulus	1000 GPa

### 2.6.1 Bending of CNT with Respect to Mechanical Properties

The strong covalent carbon-carbon bond on the tube structure, initiate the strength tube property which make it stronger than steel (Endo *et al.*, 2004). Noted that the mechanical properties of the nanotubes itself is a challenge to experimentally

study due to the difficulty in obtaining pure CNTs which is free from amorphous, graphitic, and polyhedral carbon particles (Ruoff and Lorents, 1996).

Poncharal *et al.* (1999) has demonstrated that nanotubes can bend to a certain degree when stress is applied and return to its original form after the stress is released. This behavior makes nanotubes special compared to other type of filler due to the susceptibility towards fracture when the tubes are subjected to stress beyond the elastic limit. Moreover, CNT offer ease of processing in composites especially due to the lack of breakdown during processing. This is in contrast with carbon fibers in which the fiber breakdown occurs during composite processing (Schadler *et al.*, 1998).

### **2.6.2 Electronic Structure and Electron Transport in CNT**

The electronic structure of carbon nanotubes can be either metallic or semiconducting depending on the diameter and helicity of the tubes (Saito *et al.*, 1992; Kang *et al.*, 2006). The helicity introduces significant changes in electronic density states which show the electronic character for the nanotubes. The enhanced electronic property enables ballistic transport over more than 100 nm occurs (Bernholc *et al.*, 2002).

Figure 2.10 shows the schematic image on the electron transfer in metal, semiconductor and graphite by Collins and Avouris (2000). As can be seen in Figure 2.10, there are two separate phases that is red and light blue. Red phase indicate the collection of energy states that are pack with electrons, while the light blue phase indicate the empty space for the electron to move in. For metals, the electron can

simply be transferred from the filled energy states (red) to the empty energy states (blue) because there were many electrons that can directly move to the adjacent conduction states. As for semiconductors, additional energy is needed in order to jump across the gaps to the first available conduction states (from red to blue). Finally graphite materials, usually have semimetallic conducting behavior that conduct through minimal point. Applying external boost allowing more electron to access the narrow path to the conduction state.

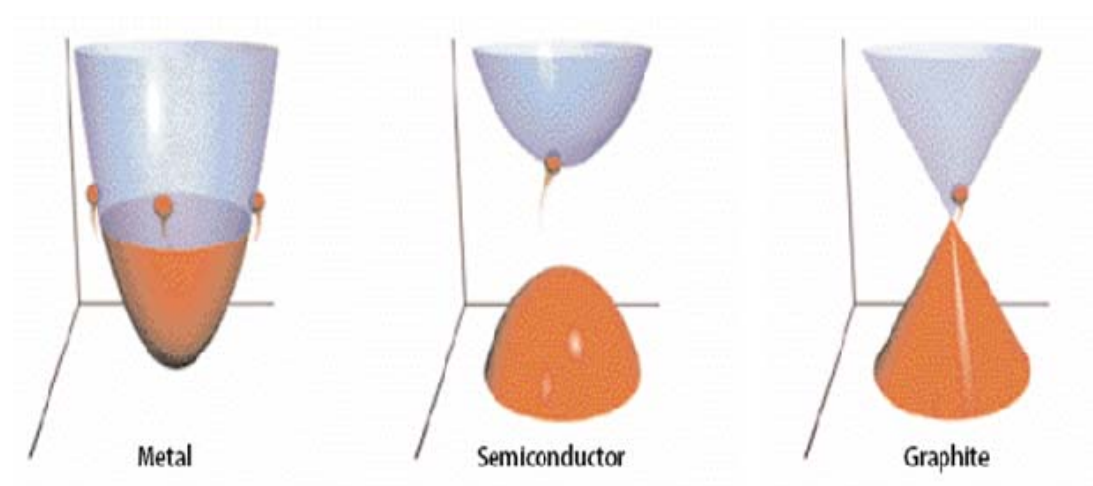


Figure 2.10 Schematic images on electron transfer in metal, semiconductor and graphite in order to determine the electrical properties of the materials (Collins and Avouris, 2000).

Figure 2.11 illustrates the semiconducting and metallic behavior of the straight and twisted nanotubes by Collins and Avouris (2000). For the straight nanotubes (Figure 2.11a), it looks like the graphite sheet (left) was rolled into the center of the tube. The nanotubes geometry limits the electron transfer and makes two thirds of nanotubes metallic while the rest one third is semiconducting. The point at which there is close contact that joins the electron with conduction states is known as Fermi point. For twisted nanotubes (Figure 2.11b), the graphite sheets were rolled into twisted dimension. The twisted nanotube allowed energy states for the electron

to have an incision at an angle resulted in one third of the nanotubes is metallic while the rest is semiconducting.

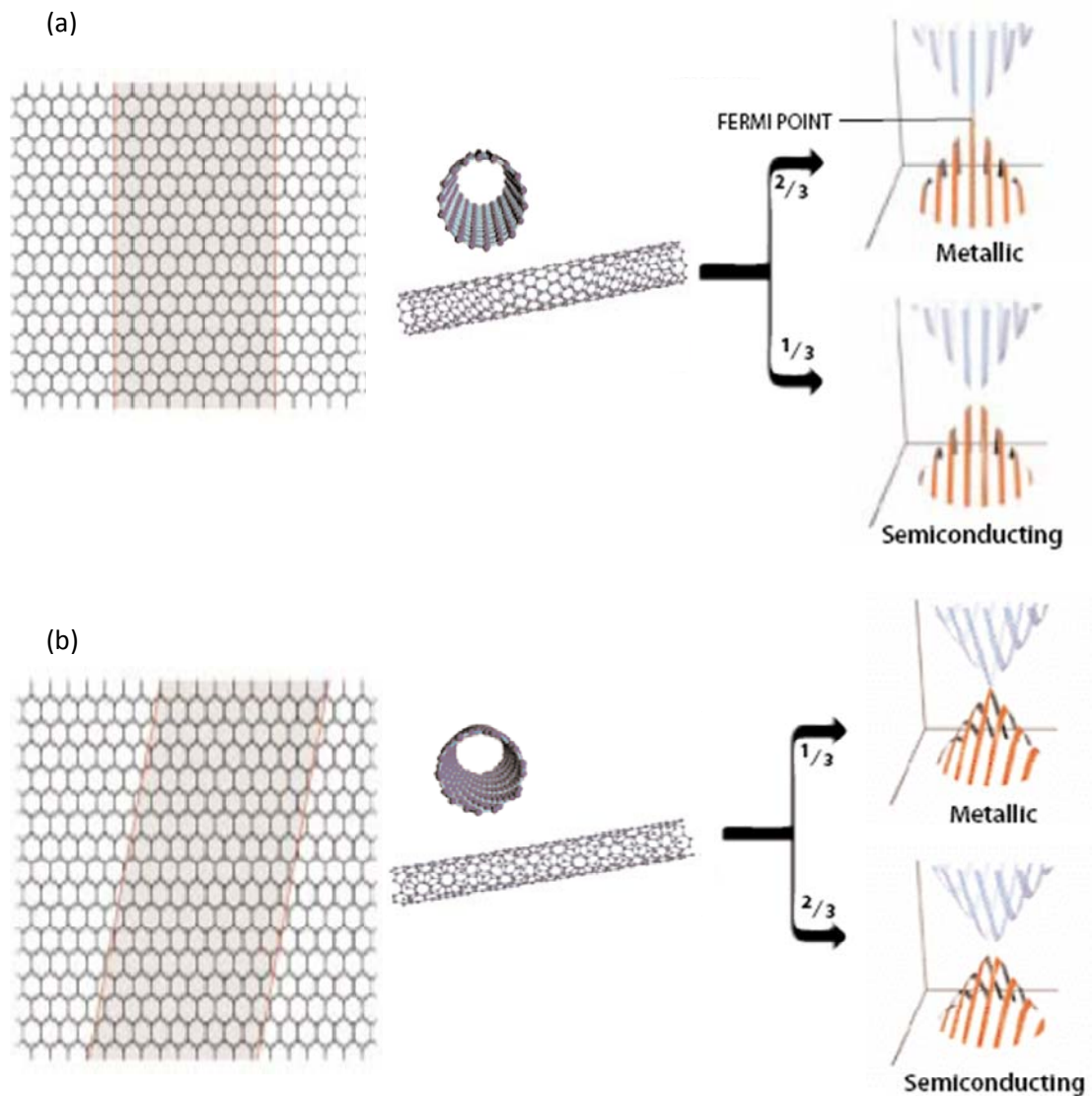


Figure 2.11 Schematic drawing on metallic and semiconducting of (a) straight nanotubes and (b) twisted nanotubes (Collins and Avouris, 2000).

Few facts need to be consider with regard to electron transport in MWCNT, i.e:

- a) the semimetallic behavior, which have drastic effect on the band structure and on the scattering mechanism.
- b) the effect of reduced dimensionality.
- c) impact on weak disorder due to the quantum aspects of conduction.

d) possibility of walls intercalation and its effects.

The MWCNT also can behave as an ultimate fiber while SWCNT can behave as pure quantum wires. It is known, MWCNT has more than one carrier, which were electrons and positive holes. The contribution of each type of carrier is important and should be taken into account (Issi and Charlier, 1999). Due to the one-dimensional electronic structure, the electronic transport in CNT occurs ballistically over the length of the tube which enabling them to carry high currents with essentially no heating (Baughman *et al.*, 2002). The electronic properties of the MWCNT are almost similar to those perfect SWCNT.

### **2.6.3 Thermal Conductivity Behavior of CNT**

Thermal conductivity of MWCNT is  $\sim 3000 \text{ W/mK}$  while SWCNT is  $\sim 6000 \text{ W/mK}$ . These indicate that CNT have very good thermal conductivity which is greater than diamond and even graphite ( $\sim 2000 \text{ W/mK}$ ). There are two possible physical mechanisms that contribute to the high thermal conduction of the CNT; i) electron-phonon interactions. This interaction mainly depends on the electronic band structure and the electron scattering process and ii) phonon-phonon interactions. This interaction depends on the vibrational modes of the lattice. At room temperature for semiconductor CNT, the phonon-phonon interaction dominate the thermal conductivity and the electron-phonon interactions only give small contribution due to the large band gap and low density of the free charge carriers. Moreover, thermal conductivity of the nanotube is more sensitive to the states with highest band velocity and the largest mean free path. The thermal conductivity along the tube axis has at least two orders of magnitude larger than normal to the tube axis. Therefore, the

thermal conductivity of SWCNT bundle or isolated MWCNT should be close to their constituents tubes, with some inter-tube thermal conduction that could occur (Sinnott and Aluru, 2006).

Even though Ijima predicted that CNT have very high thermal conductivity among all of carbon materials, the thermal conductivity of the CNT reinforced in polymer composite was low. The individual measurements of MWCNT at room temperature is approximately 3000 W/mK. However, this value was far smaller when the CNT embedded in the polymer matrix due to the interface scattering or defects present on the tube surface (Kumar *et al.*, 2007a; Huxtable *et al.*, 2003).

#### **2.6.3.1 Effects of Different Tube Length and Tubes Chirality on Thermal Conductivity of CNT**

Sinnott and Aluru (2006) reviewed effect of tube length variation on the thermal conductivity of the tubes (Figure 2.12). The thermal conductivity of the short tube that is less than few micrometers have ballistic transport features compared to the infinitely long tube. The finite size restricts the phonon motion and causes the thermal conductivity to vary with the nanotube length. In addition, tube with difference chirality and diameter, can have different thermal conductivity properties. They also reported that nanotubes with smaller diameter have radial and azimuthal components that are larger than those tubes with large diameter. For armchair and chiral SWCNT, the  $\sigma$ -bond along the circumferences are strongly strained compared to the zigzag nanotube which could limit the phonon mean free path due to the scattering effect and lower the thermal conductivity. For armchair and zigzag nanotubes, the atom chains are parallel to the tube axis while for chiral nanotubes, the atom chains are in helix position. Therefore, in chiral nanotube position, it is easy



to transfer the momentum in radial direction since axial direction would lower the thermal conductivity of the nanotubes.

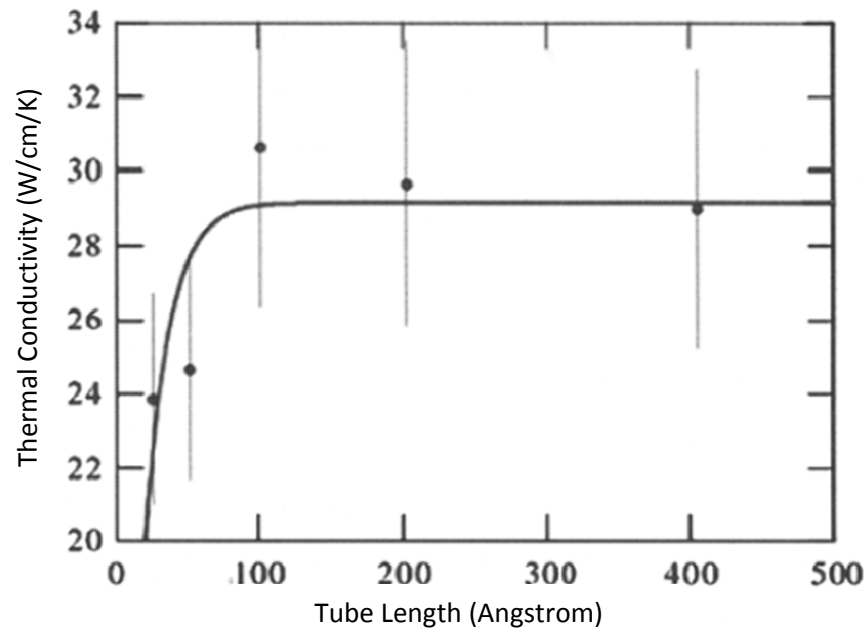


Figure 2.12 Thermal conductivity versus tube length (Sinnott and Aluru, 2006).

## 2.7 Surface Treatment on CNT

### 2.7.1 Why Surface Treatment is Important on CNT ?

The as-produced CNT has smooth tube structure. The smooth atomically tube surface with  $sp^2$  hybridized carbon structure has limited ability to form strong bonding with surrounding matrix (Barber *et al.*, 2004). Moreover, the  $\pi$ - $\pi$  interactions, long and entangled CNT tends to aggregate strongly in bundles. In addition, the tube aggregates together because of their high surface energy and van der Waals attraction between the neighboring tubes. Their long tube length make the processing become hard to control. Thus, CNTs behave as a large macromolecules and making the processing of CNTs in solvent become difficult. In fact, it is an obstacle during preparing CNT nanocomposites and furthermore, it will affect the properties of the nanocomposites produced.

Oxidation treatment on CNT surface creates some functional groups on the tube surface and cause strong interaction with matrix (Lee *et al.*, 2005). This allows the modified CNT to interact with the surrounding matrix via defects create on the nanotube surface or polymer chains wrapping around the nanotube itself. There are many evidences reported by researchers that indicate the presence of functional groups can serves as starting point for binding chemical molecules on the nanotube surfaces with surrounding matrix (Philip *et al.*, 2004; Zhang *et al.*, 2004; Zhu *et al.*, 2005; Cervini *et al.*, 2008; Ma *et al.*, 2010a).

### **2.7.2 Types of Surface Treatment on CNT**

There are two main approaches to CNT surface modification. One is covalent attachment while the other is non-covalent attachment. For noncovalent attachment, the CNT was surrounded or wrapped by polymer chain. The advantage in this type of attachment is the nature of the CNT is not altered. The disadvantage of the noncovalent attachment is the interfacial adhesion between CNT and the wrapping polymer molecule might be weak, thus stress transfer efficiency might be low. Figure 2.13 shows the example of non-covalent treatment on CNT by wrapping the hydrolyzed poly(styrene-co-maleic anhydride) (HSMA) on the CNT surface.